13th World Conference on Earthquake Engineering
Vancouver, B.C., Canada
August 1-6, 2004
Paper No. 2601

# A PROBABILISTIC APPROACH FOR SEISMIC ASSESSMENT OF R.C. STRUCTURES: APPLICATION TO HIGHWAY BRIDGES

Gianmarco de FELICE[1], Renato GIANNINI[2] and Alessandro RASULO[3]

## SUMMARY

The Effective Fragility Analysis (EFA) methodology is applied to the assessment of seismic reliability of three reinforced concrete bridges along Italian highway network. The selected bridges are different for structural scheme (continuous/simply supported deck) and pier type (single stem/frame piers). The reliability evaluation considers different sources of uncertainty: in the seismic input, through the use of different accelerograms for the dynamic analysis, in the structural behaviour, through the use of a refined non-linear finite element model, and in the ultimate state modelling. The EFA procedure implemented in this study reduces the number of simulations required for the reliability analysis using a surface response technique only for random variables affecting the structural dynamic behaviour, whilst state-limit randomness is treated explicitly during simulations. The final result of the analysis is the bridge fragility curve as function of spectral acceleration and, through its convolution with local hazard, the risk. Those results are briefly discussed with respect to the following aspects: comparison of bridge vulnerability in relation of different pier and deck structural models, influence of material randomness on final reliability, relative importance of seismic input respect to mechanical and epistemic uncertainty.

## INTRODUCTION

In this paper, the EFA reliability procedure (Effective Fragility Analysis) developed in [1] is applied to the assessment of seismic fragility of some bridges along Italian highway network. The method, modified and presented in detail in [2], is based on the different treatment of uncertainty coming from the random variables governing the dynamic response of the structure, hereafter said “external”, and from those governing the limit states for which the fragility curve is built, hereafter said “internal”.

In order to study the dependence from the external variables, collected in the vector **y**, the procedure uses the response surface method [3], [4]. This method achieves a simple functional relationship, usually of the polynomial type, between the external variables and a measure of seismic response through the run of a limited number of non-linear dynamical analysis.

[1] Associate Professor, Dipartimento di Strutture, Università degli Studi Roma Tre, Roma, Italia
[2] Professor, Dipartimento di Strutture, Università degli Studi Roma Tre, Roma, Italia
[3] Research Fellow, Dipartimento di Meccanica, Strutture, Ambiente e Territorio, Università degli Studi di Cassino, Cassino (FR), Italia

On the other hand, the dependence on the internal variables, collected in the vector **x**, do not requires the execution of extra dynamic analysis on the structure since the probability to undergo the limit state is explicitly obtained using standard reliability methods under the hypothesis of independence of collapse mechanisms.

This approach significantly reduces the number of numerical analysis required by a direct use of standard reliability techniques, like in MonteCarlo simulations.

## ANALYSIS OF EXTERNAL RANDOMNESS

The aim of the analysis is to build the seismic fragility curve of the single bridge, or, when considering also the hazard at the site, to achieve the seismic risk.

The fragility curve is obtained from the definition of the response surface of the reliability index, β, as a function of external random variables **y** representing both structural uncertainty and seismic input. Assuming a quadratic form in **y**, the response surface can be written as:

$$\beta(y) = \theta_0 + \sum_i \theta_i y_i + \sum_i \sum_j \theta_{ij} y_i y_j + \delta + \varepsilon \qquad (i,j=1,\ldots,k) \qquad (1)$$

where are present $k$+2 random variables: $k$ are required to represent the structural properties of the system, whilst the extra two variables are required to represent the input uncertainty (deriving from the fact that experiments are carried out in a not-homogeneous way due to different selection of the accelerogram in non-linear dynamic analysis) and the model error, considering all the other sources of randomness.

The definition of the unknown parameters, **θ**, is achieved through a simulation plan on **y**. The outcomes of the simulations can be expressed in a compact format as:

$$\boldsymbol{\beta} = \mathrm{Y}\boldsymbol{\theta} + \mathrm{B}\boldsymbol{\delta} + \boldsymbol{\varepsilon} \qquad (2)$$

where **β** is the vector of numerical tests, **Y** and **B** are matrices of known values, while **ε** and **δ** represent the vectors of random variables due respectively to model error and input uncertainty.

In particular **Y** is defined in accordance with the selected simulation plan on structural external variables **y** as:

$$\mathbf{Y} = \begin{bmatrix} \mathbf{v}(\mathbf{y}_1) \\ \vdots \\ \mathbf{v}(\mathbf{y}_n) \end{bmatrix}$$

where $n$ is the number of experiments and $\mathbf{v}(\mathbf{y}) = \lfloor 1 \quad y_1 \quad \cdots \quad y_m \quad y_1^2 \quad y_1 y_2 \quad \cdots \quad y_m^2 \rfloor$ is an explanatory function of the polynomial terms present in (1), whilst **B** distributes the source of input uncertainty (in our case the selected accelerograms) to the general plan of experiments.

The error terms **ε** and **δ** are modelled assuming a spherical multivariate normal distribution:

$$\boldsymbol{\varepsilon} = \mathrm{N}\left(\mathbf{0}, \sigma_\varepsilon^2 \mathbf{I}_{ne}\right), \qquad \boldsymbol{\delta} = \mathrm{N}\left(\mathbf{0}, \sigma_\delta^2 \mathbf{I}_{na}\right) \qquad (3)$$

In this case the unknowns needed in order to define the response surface are **θ**, $\sigma_\varepsilon$, $\sigma_\delta$. The problem has been solved maximizing the likelihood functional through an iterative procedure [5]:

$$L(\boldsymbol{\beta}, \mathbf{C_{YY}} \mid \mathbf{Y}) = \left|\mathbf{C_{YY}}\right|^{\frac{1}{2}} \exp\left[-(\boldsymbol{\beta} - \mathbf{Y}\boldsymbol{\theta})\mathbf{C_{YY}}(\boldsymbol{\beta} - \mathbf{Y}\boldsymbol{\theta})\right] \qquad (4)$$

where $\mathbf{C_{YY}} = \mathbf{B}\mathbf{B}^T \sigma_\delta^2 - \mathbf{I}\sigma_\varepsilon^2$ is the correlation matrix.

Numerical experiments have been planned assuming a Central Composite Design (CCD) scheme with a stellar two-level part (where the variables are changed once at one time for a total of 2$k$+1 experiments, where $k$ is the number of random variables) and a complete factorial two-level part, with $2^k$ combinations [3].

Aiming not to reproduce the same selection of structural external variables for all the accelerograms considered, a blocking technique has been used, subdividing factorial experiments in as many blocks as the number of considered accelerograms.

In the application carried out, the seismic response of the bridges has been considered affected by four external variables: three are structural: the total mass, $M$, the steel yielding tension, $f_y$, the concrete strength, $f_c$, while the fourth is a measure of the seismic input since represent the spectral acceleration at the first natural period of the structure, $S_a$, to which the examined accelerograms have been scaled.

The explicit form of response surface in this study is thus:

$$\begin{aligned}\beta = {} & \theta_0 + \theta_1 \ln(f_c) + \theta_2 \ln(f_y) + \theta_3 \ln(M) + \theta_4 \ln(S_a) + \theta_5 \ln(f_c)^2 + \theta_6 \ln(f_y)^2 + \\ & + \theta_7 \ln(M)^2 + \theta_8 \ln(S_a)^2 + \theta_9 \ln(f_c)\ln(f_y) + \theta_{10} \ln(f_c)\ln(M) + \theta_{11} \ln(f_c)\ln(S_a) + \\ & + \theta_{12} \ln(f_y)\ln(M) + \theta_{13} \ln(f_y)\ln(S_a) + \theta_{14} \ln(M)\ln(S_a) + \delta + \varepsilon\end{aligned} \tag{5}$$

where the logarithms of external variables are considered.

The seismic input is represented by the eight accelerograms reported in Table 1 and Figure 1, randomly selected from PEER database (http://peer.berkeley.edu/smcat/) with the constraint of considering intermediate soil (B type according to EC8 classification) with a magnitude in the range 6.0-7.5 and a focus-to-site distance in the range 20-40 km.

The selected time histories have been subdivided in two groups of four records each, according to the blocking scheme.

Table 1. Accelerograms used in dynamic analysis

| Id | Earthquake | Time | Station | Reg. | M | R [km] | PGA [g] | Td [s] |
|---|---|---|---|---|---|---|---|---|
| | I Group | | | | | | | |
| 1 | Chalfant Valley | 1986/07/21 14:42 | LakeCrowley - Shehorn R. | 009 | 6.2 | 36 | 0.163 | 40 |
| 2 | Cape Mendocino | 1992/04/25 18:06 | Shelter Cove Airport | 000 | 7.1 | 33.8 | 0.229 | 36 |
| 3 | Kocaeli, Turkey | 1999/08/17 | Goynuk | 000 | 7.4 | 35.5 | 0.132 | 25 |
| 4 | Loma Prieta | 1989/10/18 00:05 | Gilroy Array #7 | 090 | 6.9 | 24.2 | 0.323 | 40 |
| | II Group | | | | | | | |
| 5 | Northridge | 1994/01/17 12:31 | LA - Chalon Rd | 070 | 6.7 | 23.7 | 0.225 | 31 |
| 6 | Northridge | 1994/01/17 12:31 | LA - N Faring Rd | 090 | 6.7 | 23.9 | 0.242 | 30 |
| 7 | San Fernando | 1971/02/09 14:00 | Castaic - Old Ridge Route | 291 | 6.6 | 24.9 | 0.268 | 30 |
| 8 | Friuli, Italy | 1976/05/06 14:00 | Tolmezzo | 000 | 6.5 | - | 0.351 | 36 |

The experiment plan requires therefore repeating the 28 numerical analyses for each group with a total of 56 runs.

## LIMIT STATES AND INTERNAL RANDOMNESS

As anticipated, in this study the limit state formulation has been analysed through a function of the internal variables, **x**, where are present both the structural demand and capacity. According to the reliability procedure developed, within the numerical run the demand is a deterministic function in time $D(t)$ while the capacity can be represented as

$$C = \overline{C}(t, \mathbf{x})\,\varepsilon \tag{6}$$

where $\overline{C}(t, \mathbf{x})$ is a function of time and internal variables representing the best estimate of structural capacity, and ε is the capacity model error. In particular ε has been assumed a log-normal random variable,

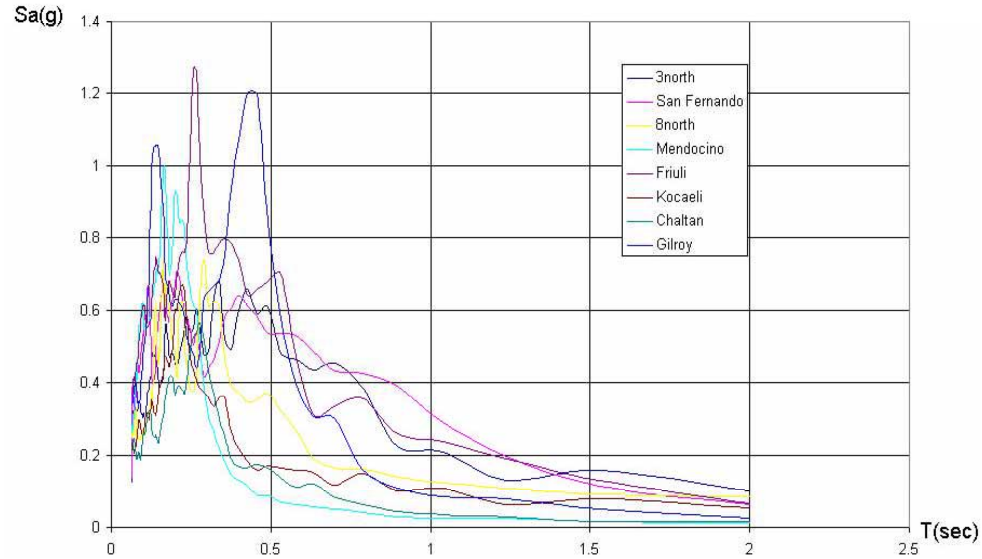


Fig 1. Response Spectra of the eight accelerograms.

with unitary mean and coefficient of variation (c.o.v.) to be selected on the basis of the model accuracy.
The limit states considered to represent the bridge pier collapse are flexure and shear.
In the flexure limit state, deformation capacity has been measured by the chord rotation $\theta$ through the expression:

$$\overline{C}_\theta = \chi_y \frac{L_s}{3} + (\chi_u - \chi_y) L_p \left(1 - \frac{L_p}{2L_s}\right) \tag{7}$$

where $\chi_u, \chi_y$ are respectively ultimate and yielding curvature of the critical section, $L_s$ is the distance from the point of counter-flexure and $L_p$ is the length of the plastic hinge. In our case the plastic hinge length has been estimated, according with [6], with the following formula:

$$L_p = 0.08 L_s + 0.22 f_y d \tag{8}$$

where the second term accounts for the strain penetration effects due to anchored longitudinal rebars (*d* is their diameter, $f_y$ their yielding strength in MPa). Equation (7) is based on a well-established model of concentrated plasticity. The choice to express the limit state in terms of chord rotation rather than in terms of section curvature is due to the aim to obtain a more stable result, not affected by possible localization of plastic deformations induced by the integration algorithm used by the computational model.
The comparison of the selected model with the result of experimental test on flexural collapse show a significant scatter inducing to select a high error term $\varepsilon_\theta$ expressed by a c.o.v. equal to 0.5.
Equation (7) can also be rewritten in a more general form in order to include the eventual yielding of the section at the other side of the element, and therefore reads:

$$\overline{C}_\theta = \left| \chi_y \frac{L}{4} + (\chi_u - \chi_y) L_p \left(1 - \frac{3L_p}{L}\right) \right| \tag{9}$$

but in this case the demand term has to be expressed as: $D_\theta = \left|\theta_i + \theta_j / 2\right|$ , where $\theta_i, \theta_j$ are respectively the chord rotations of the section under study and the one at the other end of the structural element of length *L*.

For what concerns the shear limit state, the capacity model is the one presented in [7] with the modifications suggested in [8]. For this limit state the demand is represented by the shear carried by the pier. Accordingly the capacity is expressed by the following expression:

$$\mathrm{C_V} = \left\{\mathrm{V_C}(t) + \mathrm{V_S} + \mathrm{V_N}(t)\right\}\varepsilon_V \tag{10}$$

again given as a the product of a best estimate of capacity times an error term due to model accuracy. Shear capacity here is the sum of three main contributions:

$$\mathrm{V_C} = 0.8 A_g k(t)\sqrt{f_c}\ ;\ \ \mathrm{V_S} = \frac{A_{sw}}{s} f_y D \cot(30°)\ ;\ \ \mathrm{V_N} = N \tan\alpha(t) \tag{11}$$

representing respectively the effect due to the concrete in tension, the transversal reinforcement and the presence of an arch action activated by the axial load.

In equation (11) the meaning of variables is the following: $A_g$ is the shear effective area, $f_c$ is the concrete strength, $k(t)=k(\mu(\mathrm{t}))$ is a coefficient accounting for the decrease of concrete contribution with ductility $\mu$, $A_{sw}$ is the transversal reinforcement area, *s* the stirrup distance, $f_y$ is the steel yielding strength, *D* is the net length of concrete in tension measured in the direction of shear stress, *N* is the axial load and $\alpha(t)$ is the angle between the compression strut and the axis of the element.

Curvature ductility demand can be computed as a function of yielding curvature $\chi_y$ , end rotations of the structural element, $\theta_i, \theta_j$ , of element length *L*, distance of the critical section from point of counterflexure and plastic hinge length, $L_p$ :

$$\mu = 1 + \frac{\left|\theta_i + \theta_j / 2\right|}{\chi_y L_p^*} - \frac{L}{L_p^*}; \tag{12}$$

where $L_p^* = L_p\left(1 - \frac{3L_p}{4L_s}\right)$.

According on a limited number of experimental/theoretical comparison carried out by the shear model developers [8], the error term, $\varepsilon_V$, c.o.v. has been assumed equal to 0.3.

Table 2. Internal random variables and log-normal parameters

| No | Random Varaiable | | μ | c.o.v. |
|---|---|---|---|---|
| 1 | $\varepsilon_\theta$ | Model error for flexural Limit State | 1 | 0.5 |
| 2 | $\varepsilon_V$ | Model error for shear Limit State | 1 | 0.3 |
| 3 | $\varepsilon_{\chi_y}$ | Yielding curvature | 1 | 0.1 |
| 4 | $\varepsilon_{\chi_u}$ | Ultimate curvature | 1 | 0.1 |
| 5 | $\varepsilon_{L_p}$ | Plastic hinge length | 1 | 0.3 |

Aside the $\varepsilon_\theta$ and $\varepsilon_V$ model errors, the ultimate and yielding curvatures of critical sections $\chi_u, \chi_y$ and the plastic hinge length, $L_p$, have been treated as internal random variables in order to represent uncertainties on the estimates of their value, especially the plastic hinge length that has to be considered as a conventional rather than a physical quantity. In all the above cases randomness has been treated assuming the parameter as a best estimate value times a log-normal fluctuation with a given c.o.v. as reported in Table 2.

## THE VALLONE DEL DUCA VIADUCT

The viaduct is along the highway A16 Napoli-Canosa, in the Southern Italy, between Benevento and Avellino. The bridge has been recently retrofitted restraining the deck gaps and introducing seismic isolators at pier caps, but has been studied in the 'as built' conditions.

The bridge has 6 spans, each 32 m long with a structural scheme of a simple supported beam. The deck is composed by three pre-stressed beams 1.92 m high, connected by 5 traversal link and a slab 20 cm thick and 9.54 m wide. The r.c. piers have a single stem with a rectangular solid section $1.40 \times 2.70$ m and a total longitudinal reinforcement of 40 rebars $\phi 28$.

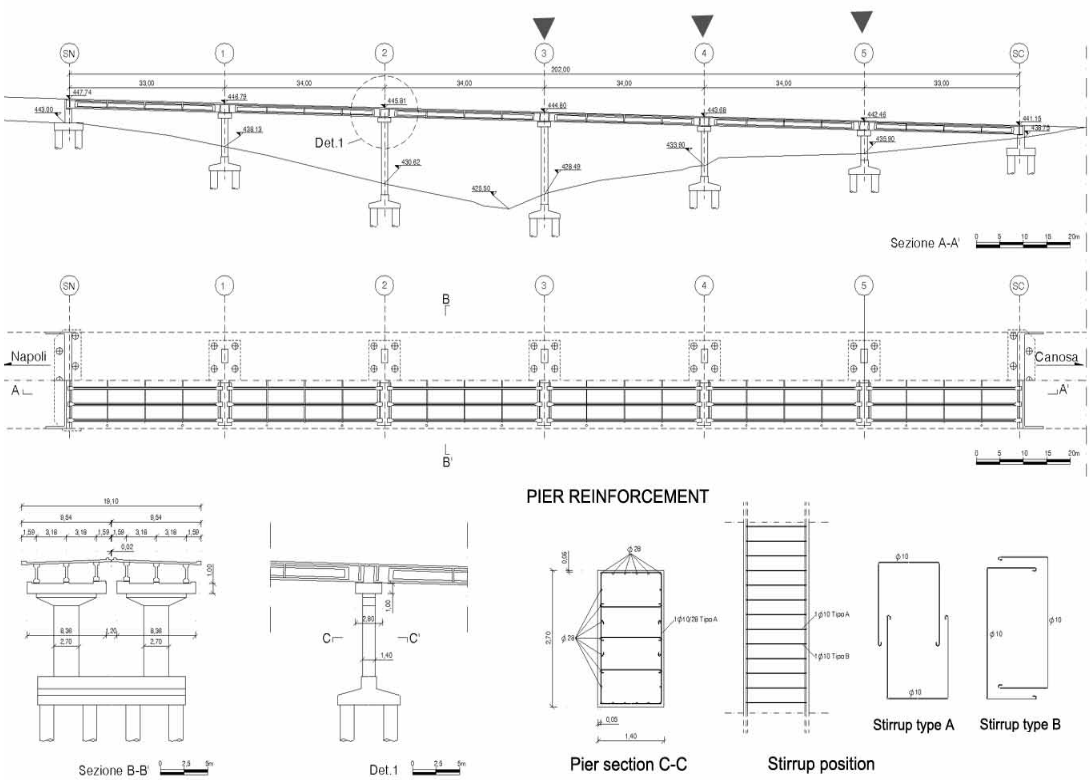


Figure 2. Vallone Del Duca viaduct.

Mechanical properties of materials have been obtained from the original design documentation and from experimental test carried out when the retrofitted was planned.

Concrete strength, on the basis of core samplings at pier base, has been evaluate on average about $\bar{f}_c = 45\,\text{MPa}$ and c.o.v. equal to 0.17. The reinforcing steel is classified Aq50, a mild steel type following old Italian regulation (Circolare Min. LLPP N. 1472 del 1957) with an ultimate strength not less than 500 MPa, an yielding strength not less than 270 MPa and a ultimate strain not less than 16%. Statistical studies on Aq50 grade steel permit to evaluate average strength and c.o.v. both at yielding: $\bar{f}_y = 370\,\text{MPa} \quad \text{c.o.v.} = 0.08$, and at ultimate $\bar{f}_u = 545\,\text{MPa} \quad \text{c.o.v.} = 0.05$.

In the following the reliability results for three piers are illustrated (see Fig. 2), namely n° 3, 16 m height, n° 4, 9.5 m height and n° 5, 5.5 m height.

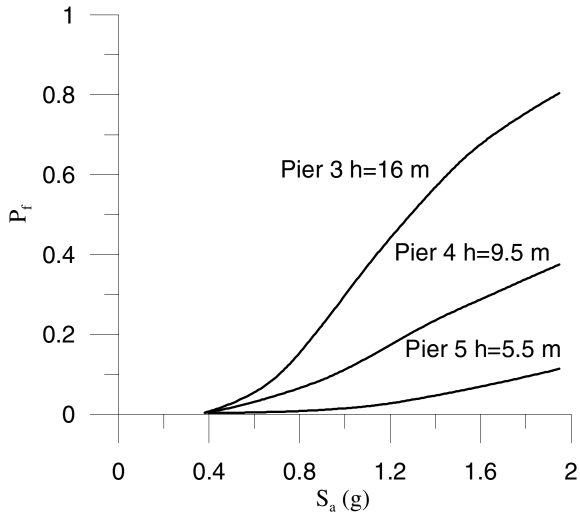


Fig. 3 Fragility curves of three pier of Vallone del Duca via-

The final result, in terms of fragility curve, is illustrated in Fig. 3. The differences can be explained since in pier 5, the squattest, failure is reached essentially in shear with a strong correlation of $f_c$ on failure probability, whilst in pier 3, the more slender, failure is reached essentially in flexure.
The comparison of fragility curves shows that most vulnerable pier is the tallest. Convolving the fragility of that pier with the seismic hazard at site we obtain a probability of collapse evaluated in 100 years equal to 2.2%.

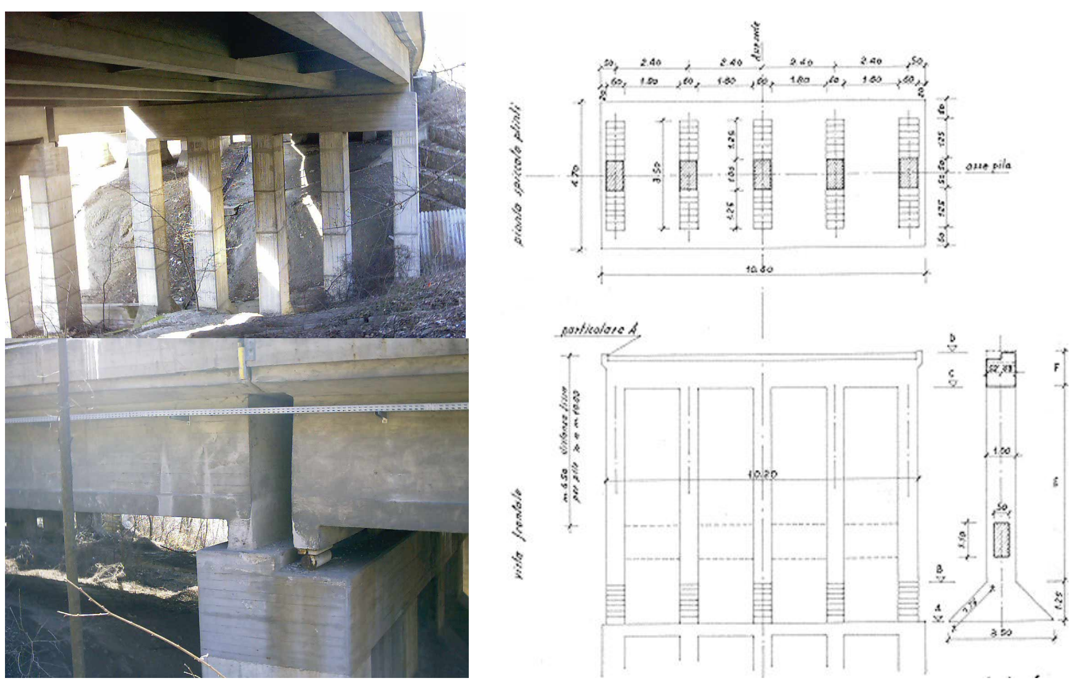

Fig. 4 The Olmeta Viaduct

## THE OLMETA VIADUCT

The Olmeta viaduct (see Fig.4) is along A1 highway between Bologna and Florence, in the Central Italy. It has been built during early ’60, without seismic provisions. The deck has five pre-stressed beams with a span 21.16 m long and a slab 9.60 m wide excluding sidewalks about 70 cm wide. The piers have a framed structure with five columns with a section 100 × 60 cm each and a spacing of 2.40 m among them, linked together by a cap beam with a section 100 × 110 cm. The pier height varies to a maximum of 12 m. The deck is simply supported by piers. Pier reinforcement consists of 12 rebars ϕ16 longitudinally and

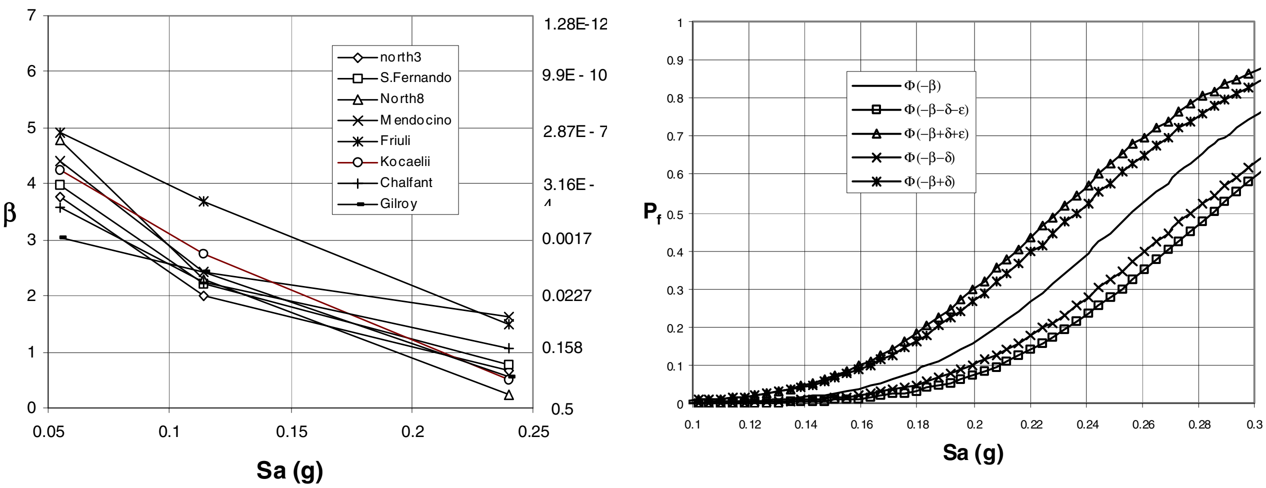


Fig. 5 Olmeta viaduct, pier n. 2: (left) Reliability index β for different accelerograms vs. the spectral acceleration; (right) Fragility curve and sensitivity of error model and variability of response.

ϕ10 stirrups every 16 cm transversally.

In 1974 the viaduct has been retrofitted: slab has been rebuilt and pier columns have been jacketed by a 10 cm thick concrete layer reinforced longitudinally by 6 rebars ϕ20 and transversally by ϕ10 stirrups every 40 cm, but the analysis has been carried out in the ‘as built’ status.

In the following the results are reported only for pier n°2 (column 9 m high).

Figure 5 (left) sows the variability of the reliability index evaluated in the central point of the experiment design for the different accelerograms used in the analysis; the plots in figure 5 (right) show the fragility curve of pier n°2 and the influence of model errors and of the spread of response evaluated at ± one standard deviation of r.v. ε and δ.

## THE CADRAMAZZO VIADUCT

The Cadramazzo viaduct is along highway A23 between Udine and Tarvisio, in North of Italy, and has been built after the Friuli earthquake according to some seismic regulation developed at that time. The viaduct has a continuous deck for a total of 15 spans each of them 40 m long. The deck is constituted by a prestressed multicellular section stiffened by transversal beams at supports on piers. Piers have a circular hollow section with a 3.8 m external diameter and different heights ranging from 3 to 24.9 m. Tall piers have an initially solid section for a length of 2.5 m that becomes hollow at higher levels with a concrete thickness different for each pier, but in the range 50-65 cm.

Seismic reliability of the pier has been considered only in the transversal direction (orthogonal to bridge axis). In the numerical model material inelasticity has been considered only in the piers, while cap beams

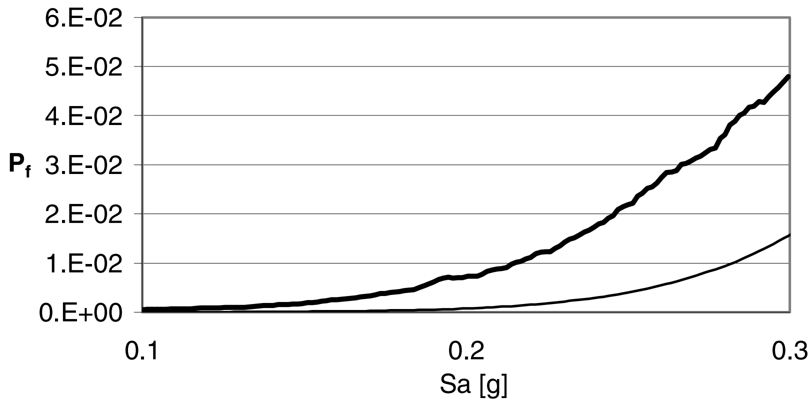


Fig. 6 Cadramazzo viaduct: fragility of the bridge (thick line) and probability of failure at the central point of experiment design (thin line)

and deck have been modelled through elastic models. Supporting devices at the interface between pier and deck have been modelled using neoprene elastic properties.

Material properties have been assumed according to values reported on original design documentation as follows: concrete has an average strength $\bar{f}_c = 34.11\,\text{Mpa}$ and a c.o.v. equal to 0.27, whilst steel has an average yielding strength $\bar{f}_y = 430\,\text{Mpa}$ and a c.o.v. equal to 0.09.

Figure 7 shows fragility curve of the whole viaduct (thick line) compared to the one calculated on the basis of median value of random variables (thin line). The differences between the two curves measures the relevance due to structural random variables.

## CONCLUSIONS

The risk assessment procedure developed for concrete structures has been applied to three highway Italian viaducts, assumed to represent typical cases for diffusion of structural scheme. Two are simply supported by single stem or frame piers, the third is a continuous bridge. The bridges have been modelled with a refined finite element analysis program [9] and different collapse mechanism have been considered.

The results obtained proof not only the effectiveness, but also the flexibility of the reliability technique implemented. Indeed complex structures have been analysed using realistic models for actions and capacity, including the associated uncertainties that, as shown in Fig. 6, have a relevant effect on final value of fragility. Finally it has been possible to derive the sensitivity of failure risk upon single random variables, in order to plan a rational retrofit strategy.

## REFERENCES

1. Giannini R., Pinto P.E., de Felice G. “Seismic reliability assessment of RC structures”. Submitted to *Asce Jorunal of Structural Engineering*, 2003.
1. de Felice G., Giannini R. “A probabilistic approach for seismic assessment of r.c. structures: Theory”. *13$^{th}$ WCEE*, Vancouver, Canada. Paper no. 2600, 2004.
2. Box G.E.P., Draper N.R. *Empirical Model-Building and Response Surfaces*, John Wiley & Sons, 1987.
3. Franchin P., Lupoi A., Pinto P.E. “Seismic fragility of reinforced concrete structures using a response surface approach”. *Journal of Earthquake Engineering,* 2003, **7**: 45-77.
4. Searle S.R., Casella G., McCulloch C.E. *Variance Components,* Prentice-Hall, 1992.

5. Priestley M.J.N., Seible F., Calvi G.M. "*Seismic Design and Retrofit of Bridges"*, John Wiley & Sons, 1996.
6. Priestley M.J.N., Verma R., Xiao Y. "Seismic shear strength of reinforced concrete columns". *ASCE Journal of Structural Engineering,* 1994, **120** (8): 2310-2329.
7. Kowalsky M.J., Priestley M.J.N. "Improved analytical model for shear strength of circular reinforced concrete columns in seismic regions". *ACI Structural Journal,* 2000, **97**( 3): 388-396.
8. Petrangeli M., Pinto P.E., Ciampi V. "Fibre Element for cyclic bending and shear of RC structures. I: Theory", *ASCE Journal of Structural Engineering*, 1999, **125**(9): 944-1001.